International Conference on Space Optics—ICSO 2008

Toulouse, France

14–17 October 2008

Edited by Josiane Costeraste, Errico Armandillo, and Nikos Karafolas

Innovative design of EUV multilayer reflective coating for improved spectral filtering in solar imaging

Michele Suman

Maria Guglielmina Pelizzo

David L. Windt

Gianni Monaco

Sara Zuccon

Piergiorgio Nicolosi

International Conference on Space Optics — ICSO 2008, edited by Josiane Costeraste, Errico Armandillo, Nikos Karafolas,
Proc. of SPIE Vol. 10566, 1056667 · © 2019 SPIE · CCC code: 0277-786X/19/$21 · doi: 10.1117/12.2584165

INNOVATIVE DESIGN OF EUV MULTILAYER REFLECTIVE COATING FOR IMPROVED SPECTRAL FILTERING IN SOLAR IMAGING

Michele Suman,[1,2]

Maria Guglielmina Pelizzo,[1] David L. Windt,[3] Gianni Monaco,[1,2] Sara Zuccon,[1,2] and Piergiorgio Nicolosi,[1,2]

1. *Information Engineering Department, University of Padova, via Gradenigo 6B, Padova, 35131 Italy CNR-INFM – Laboratory LUXOR, via Gradenigo 6/b – 35131 Padova (Italy)*
2. *National Research Council- National Institute for the Physics of the Matter, LUXOR Laboratory, via Gradenigo 6B, Padova, 35131 Italy*
3. *Reflective X-ray Optics LLC, 1361 Amsterdam Ave., Suite 3B, New York, NY 10027, USA*

Corresponding author: sumanmic@dei.unipd.it

ABSTRACT

Space optic instrumentation for the sun observation in the Extreme Ultraviolet (EUV) spectral region is often based on multilayer coating technology. Such coatings have not negligible bandwidth, and therefore, often the detected signal is due to the contribution of different very close spectral lines. In this work we present a study of innovative capping layer structures covering the multilayer coating able to improve the rejection of the unwanted lines and at the same time preserving the reflectivity peak at the working wavelength.

1. INTRODUCTION

In recent years telescopes based on near normal-incidence multilayer mirror technology have been employed in many missions dedicated to the Sun observation in EUV wavelengths, as in particular Fe-IX (17.1 nm), Fe-XII (19.5 nm), Fe-XV (28.4 nm) and He-II (30.4 nm). Examples of successful missions are SOHO (EIT) [1] and TRACE [2]. Performance of multilayer are mainly evaluated in terms of peak reflectivity at working wavelength and rejection capability of unwanted lines.

Because of their good time stability, Mo/Si multilayer are conventionally used for all of these wavelengths, even if, at the longer ones they have relatively low reflectivity peak with respect to other material couples. Moreover, in the case of a Mo/Si periodic structure optimized for 28.4 nm, the reflectivity curve is quite spectrally broad and includes the strong HeII line, that can affect diagnostic with the Fe line signal. A suitable narrowband solution which cuts down the HeII reflection has been obtained through an a-periodic ML structure design [3]. Moreover, further enhancement of peak reflectivity can be obtained using other material combinations like Mg/SiC [4], B_4C/Si/Mo [5] or B_4C/Si [4]. Although for some of these structures, test and proof of lifetime stability must be investigated.

We propose an innovative method for designing suitable capping layer covering the multilayer structure which do not affect the reflectivity peak while rejecting unwanted emission, for example from relatively close lines. The capping layer solution can be adopted both in case of periodic and a-periodic multilayer, made by different materials. The capping layer can be realized using a ML structure of different materials, for example to get additional mechanical or optical properties, as the capability of surviving in harsh environmental space conditions or to suitably reject visible/UV spectral ranges.

In this paper we present and discuss theoretical results for some structures designed by the use of the new mathematical tool. Experimental results related to periodic Mo/Si multilayer covered by an optimized Mo/Si capping layer able to reflect the Fe-XV line with rejection ratio of some orders of magnitude for the near He-II intense line are presented.

In section 2 a theoretical analysis of the capping layer design is exposed, in section 3 some theoretical results are discussed. In section 4 preliminary experimental results are presented.

2. ANALYTICAL DESIGN METHOD

The innovative basic idea is to take advantage of the e.m. field standing wave configuration generated in the multilayer structure by the superposition of incident and reflected fields. As already pointed out in [6], the last protective layer in a ML structure can be grown at the node-position of the standing wave field intensity distribution in the ML. In fact, by suitable design of the last uppermost layers it is possible to shift the standing wave distribution at the top of the ML. In this way the performance of the structure result essentially insensitive to the cap-layer characteristics.

Let's now consider two wavelengths, the first λ_{peak} is the "useful" wavelength and the second λ_{noise} is the wavelength to be rejected. ML (multilayer) is the coating sub-structure constituted by the repetition of

two or more materials designed in order to obtain the best reflectivity peak at the λ_{peak} wavelength and CL (capping layer) is the structure made of last layers covering the ML, which is designed in order to preserve the λ_{peak} wavelength signal and suppress the λ_{noise} wavelength signal (see Fig. 1).

The CL structure, like the ML structure, is constituted by a sequence of absorber and spacer materials (see Fig. 1), the materials can be the same or different from the ones in the ML, in any case their thickness must be suitably optimized.

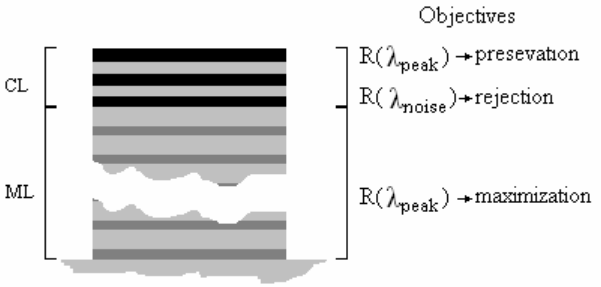

Fig. 1 A schematic view of the conceptual subdivision between CL and ML and of their performance.

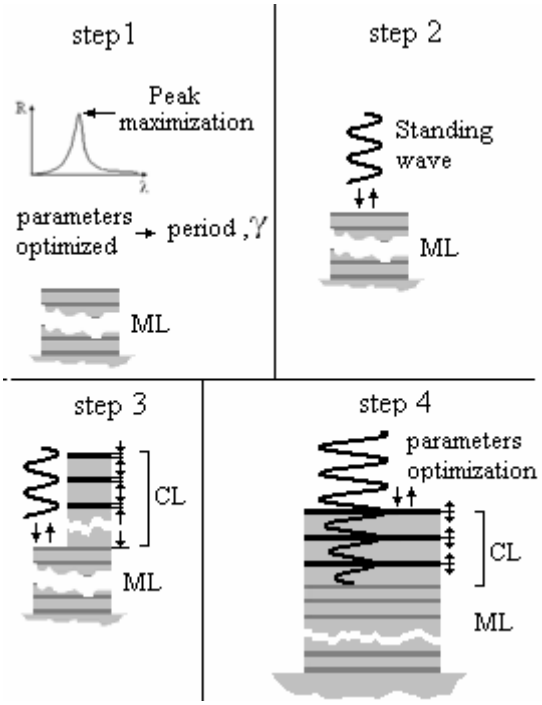

Fig. 2 A schematic of the sequence of steps followed for the multilayer optimization, here , for clarity, only the standing wave at λ_{peak} is shown. Step 1, ML design; step 2, Fields computation; step 3, CL design; step 4, optimization.

The optimization design sequence of an optimal structure consists of the following steps (see Fig. 2):

1) design of the ML (periodic or a-periodic) in order to have the maximum reflectivity peak at λ_{peak}
2) computation of the standing wave in the ML structure for λ_{peak} wavelength, and also computation of the standing wave in the ML structure at λ_{noise} wavelength
3) optimization of the thicknesses and the number of the CL layers by growing the absorber layers into the λ_{peak} standing wave nodes in order to preserve the reflectivity at the λ_{peak} wavelength and as close as possible to the anti-nodes of the λ_{noise} standing wave in order to efficiently reject the contribution at this wavelength
4) finally we optimize the CL layers and the ML period and γ parameters in order to improve the ratio $R(\lambda_{peak})/R(\lambda_{noise})$ while keeping high peak reflectivity.

By Positioning the absorber layers into the standing wave node we minimize the detrimental radiation extinction effect at the λ_{peak} wavelength almost preserving the same reflectivity peak of the ML structure. At the same time, due to the different standing wave behavior at different wavelengths, we can have an higher radiation extinction at the λ_{noise} wavelength than at the λ_{peak} one.

3. SIMULATION OF SOME APPLICATIONS

Different structures have been designed for reflecting the 33.5 nm or the 28.4 nm lines while rejecting the strong 30.4 nm one. These structures are based on Mo/Si ML structures with different CL, and are reported in Table 1. In this section we show and discuss the theoretical simulations, performed with IMD program [7]. The considered cases can be very interesting for example for GOES-R mission [8].

Case	ML materials	CL materials	λ_{peak}	λ_{noise}
1	Mo/Si	W/Si	33.5	30.4
2	Mo/Si	Pt/Si	28.4	30.4
3	Mo/Si	Cr/Si	28.4	30.4
4	Mo/Si	Mo/Si	28.4	30.4

Table 1: column 1, the index of the different cases, column 2 and 3, respectively the ML and CL materials, in column 4 and 5, respectively the λ_{peak} and λ_{noise} wavelengths in nm.

3.1 Case 1

Mo/Si ML with W/Si CL working at 33.5 nm with high rejection at 30.4 nm have been designed. The W absorption coefficient is reported in Fig. 3, it shows a very high extinction at both wavelengths of interest, in addition thin W layer deposition has been already tested for ML structures for X-ray mirrors.

In Table 2 the structure of the optimized multilayer is reported. In Table 3 and in Fig. 4 the performance of

the optimized structure is compared with the performance of a standard Mo/Si periodic multilayer. The new design shows a peak reflectivity loss of 2.6% in absolute percentage with respect to the standard periodic ML but with a considerably improved, about two orders of magnitude, rejection ratio.

CL Structure	Value
W	2.0 nm
a-Si	16.5 nm
W	2.2 nm
a-Si	16.5 nm
W	2.0 nm
ML structure	Value
Period (a-Si/Mo)	18.2 nm
Ratio	0.89
Period number	35

Table 2 The structure of the optimized multilayer for case 1.

	$R_{33.5\ nm}$	$R_{30.4\ nm}$
Standard periodic	0.197	0.044
Optimized ML+W/Si CL	0.171	$1.79*10^{-4}$

Table 3 Columns 2 and 3, respectively the reflectivity at the λ_{peak} and λ_{noise} wavelengths for the case 1.

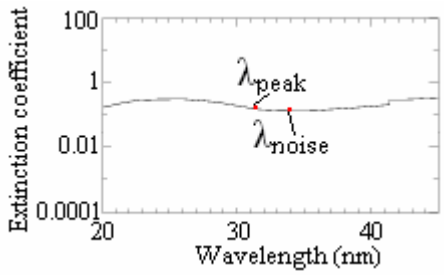

Fig. 3 The behavior of the W extinction coefficient in the 20-45 nm spectral range.

3.2 Case 2

The next three cases are based on Mo/Si ML structures with different CL, designed in order to reflect at 28.4 nm with the highest rejection at 30.4 nm.

In this case a Pt/Si CL has been designed. Pt has been chosen because it is a very suitable CL absorber material for this spectral region (see Fig. 5).

The structure is reported in Table 4, in Table 5 and in Fig. 6 the performance of the optimized multilayer are compared with a Mo/Si periodic multilayer designed in

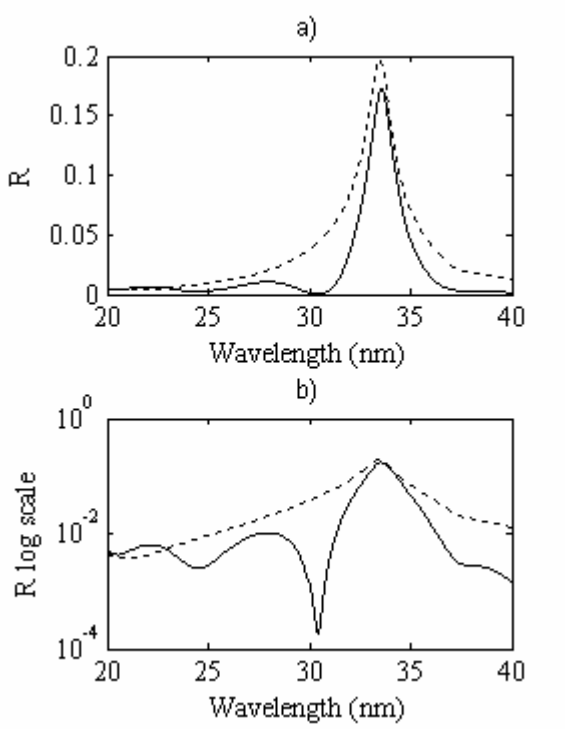

Fig. 4 In the case a) The reflectivity behavior of the optimized multilayer with a W/Si CL, continuous curve, compared with the performance, dashed line, of a standard periodic multilayer optimized only for the λ_{peak} wavelength. In the case b) the same data of the case a) reported in log scale. The reflectivity is optimized and calculated at 5° normal incidence.

CL Structure	Value
Pt	2.2 nm
a-Si	13.4 nm
Pt	2.0 nm
a-Si	12.8 nm
Pt	2.0 nm
a-Si	11.6 nm
Mo	2.0 nm
ML structure	Value
Period (a-Si/Mo)	15.3 nm
Ratio	0.87
Period number	35

Table 4. The structure of the optimized multilayer for case 2.

	$R_{28.4\ nm}$	$R_{30.4\ nm}$
Standard periodic	0.25	0.045
Optimized ML + Pt/Si CL	0.21	$6.7*10^{-5}$
Optimized ML + Cr/Si CL	0.2	$3*10^{-5}$
Optimized ML + Mo/Si CL	0.196	$2.62*10^{-5}$

Table 5 Columns 2 and 3, respectively the reflectivity at the λ_{peak} and λ_{noise} wavelengths for cases 2,3,4.

order to reflect the 28.4 nm wavelength. In this case we have obtained a reflectivity loss of 4% in absolute percentage but with improved rejection of about three orders of magnitude.

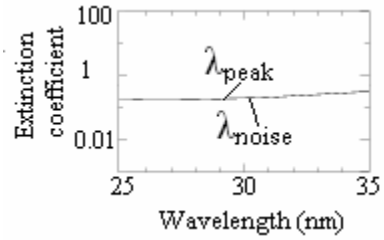

Fig. 5 Pt extinction coefficient in the 25-35 nm spectral range.

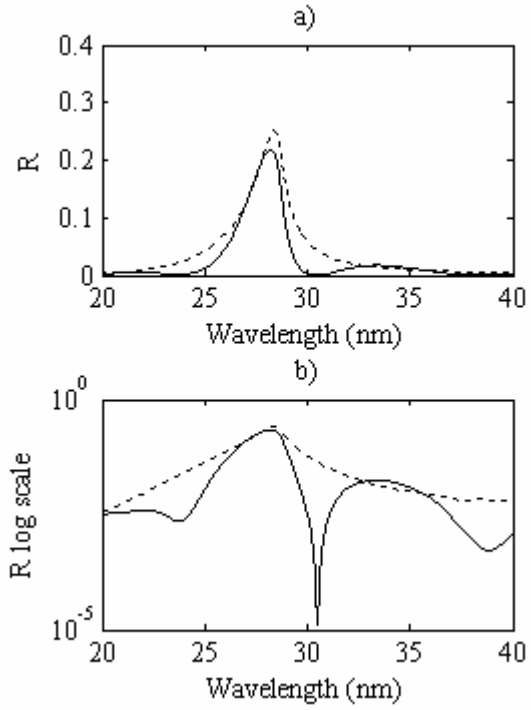

Fig. 6 In the case a) The reflectivity behavior of the optimized multilayer with a Pt/Si CL, continuous curve, compared, with a standard periodic multilayer optimized for the λ_{peak} wavelength, dashed line. In the case b) the same data of the case a) reported in log scale. The reflectivity is optimized and calculated at 5° normal incidence.

3.3 Case 3

The next two cases have been chosen in order to have an easier deposition procedure, i.e. with a lower number of sputtering target materials.

In this case a Cr/Si CL has been adopted. A Cr adhesion layer between the substrate and the multilayer can be grown in order to avoid any adhesion failures, moreover, the Cr layer tends to absorb surface contaminants on the substrate, and it also has tensile stress which balances the large compressive stresses in the multilayer. The high stress in the multilayer is due to high gamma ratio (γ) value of the Si/Mo coatings optimized for this spectral region.

In this case the Cr material has been used both like CL absorber layer and adhesion layer, this in order to permit the deposition of an optimized multilayer structure by utilizing a magnetron sputtering deposition system with only three cathodes.

Cr doesn't show the best property as candidate for the CL structure, in particular the absorption is lower than for the Pt or Mo cases. For this reason in the optimization process the Cr layers are slightly displaced with respect to the 28.4 nm standing wave nodes. The new positions give the best ratio value between the standing wave area into the CL structure at the 28.4 nm and 30.4 nm wavelengths.

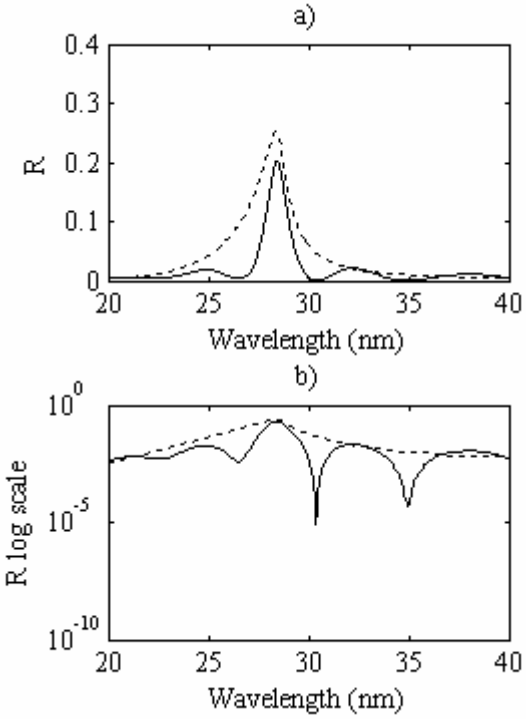

Fig. 7 In the case a) The reflectivity behavior of the optimized multilayer with a Cr/Si CL, continuous curve, compared with, a standard periodic multilayer optimized for the λ_{peak} wavelength, in dashed line. In the case b) the same data of the case a) reported in log scale. The reflectivity are optimized and calculated at 5° normal incidence.

The resulting structure is reported in Table 6, we highlight the high number of CL layers necessary to obtain a high enough rejection, due to the low absorption of Cr. The resulting performance is reported in Table 5 and in Fig. 7

CL Structure	Value
Cr	3.2 nm
a-Si	12.3 nm
Cr	3.05 nm
a-Si	12.6 nm
Cr	2.9 nm
a-Si	12.8 nm
Cr	2.7 nm
a-Si	13.1 nm
Cr	2.5 nm
a-Si	12.1 nm
Mo	2.0 nm
ML structure	Value
Period (a-Si/Mo)	15.2 nm
Ratio	0.87
Period number	35

Table 6 The structure of the optimized multilayer for case 3.

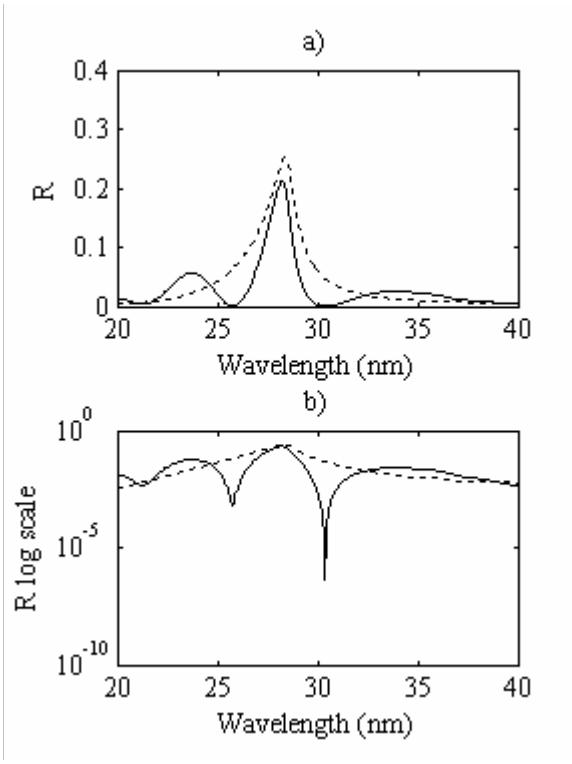

Fig. 8 In the case a) The reflectivity behavior of the optimized multilayer with a Mo/Si CL, continuous curve, compared with the performance, of a standard periodic multilayer optimized for the λ_{peak} wavelength, dashed line . In the case b) the same data of the case a) reported in log scale. The reflectivity are optimized and calculated at 5° normal incidence.

3.4 Case 4

In this last case only Mo and Si have been taken into account as possible materials both for the ML and CL structures.

Mo has a relevant absorption coefficient in this spectral region, it assures a good time stability coupled with Si, only one Mo layer for the CL structure placed in an optimal position that corresponds to a standing wave node for the 28.4 nm wavelength and standing wave anti-node for the 30.4 nm wavelength has been chosen. The multilayer structure is shown in Table 7, in Table 5 and in Fig. 8 the optimized multilayer performance is compared with the standard periodic multilayer.

CL Structure	Value
a-Si	14.7 nm
Mo	2.2 nm
a-Si	57.75 nm
Mo	2 nm
ML structure	Value
Period (a-Si/Mo)	15.15 nm
Ratio	0.868
Period number	35

Table 7 The structure of the optimized multilayer for case 4.

4. EXPERIMENTAL RESULTS

CL Structure	Value
a-Si	15.4 nm
Mo	3.55 nm
a-Si	41.2 nm
Mo	3.55 nm
ML structure	Value
Period (a-Si/Mo)	15.3 nm
Ratio	0.768
Period number	40

Table 8 The structure of the re-designed multilayer using optical constants of Tarrio et al.[9], see text.

In this section preliminary experimental results are presented. Samples deposition has been performed at RXO with magnetron sputtering technique. Preliminary tests have shown that samples with structure as for case 3, Mo/Si ML + Cr/Si CL, are quite critical. In fact the resulting performance can be very sensitive to manufacturing tolerances, due to the relatively high number of Cr layers; even a small error in the various layer thickness can result in a not negligible displacement of the Cr layers with respect to the standing wave field distribution. Furthermore preliminary experimental tests have shown that the ML+CL structure performance is also critically dependent on the optical constants of materials, accordingly an optimized structure design has been derived using the optical constants experimentally measured and reported by Tarrio et al. [9]. The corresponding Mo/Si multilayer with Mo/Si CL structure is reported in Table 8. A prototype of this sample has been deposited (RXO) and tested. The reflectivity has been measured with a laser plasma facility [10].

In Fig. 9 the experimental results for the a-periodic optimized structure, dotted curve, compared with the theoretical simulation, dashed curve, and those computed for a standard periodic structure, continuous curve, are reported.

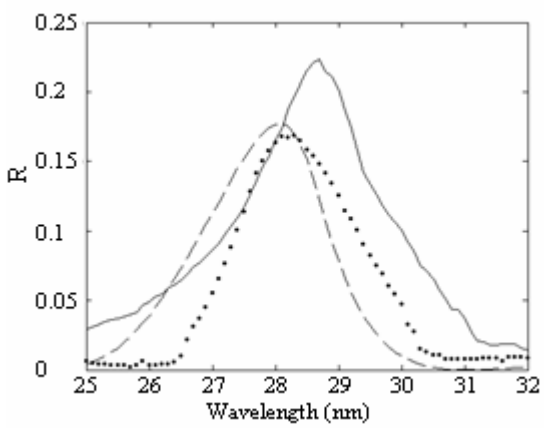

Fig. 9 Experimental results for the a-periodic optimized structure (dotted curve), compared with the theoretical simulation (dashed curve), and those computed for a standard periodic structure (continuous curve).

The good agreement between theoretical and experimental results is noticeable. Simulations show that the critical parameter of this multilayer is the thickness of the second 41.2 nm thick Si layer, a relative error of only a few percent can affect considerably the final performance, resulting in lower reflectivity peak and shifting of peak and rejected wavelengths. From these preliminary measurements the good agreement between the theoretical and experimental reflectivity wavelength peak confirms the high accuracy of this critical layer.

Further measurements are planned at ALS synchrotron in order to accurately measure the rejection ratio at the 30.4 nm wavelength, the measurements here reported are, in fact, limited by the signal to noise ratio.

5. CONCLUSIONS

We have presented an innovative method for the design of multilayer structures with improved spectral filtering performance. Structures with high rejection at the strong 30.4nm HeII line have been designed. Preliminary samples have been realized and tested, obtaining good agreement with simulations and demonstrating actual feasibility.

6. ACKNOWLEDGEMENTS

This work has been supported by ASI grant n. I/015/07/0.
The work has been performed also in the framework of the COST ACTION MP0601 "Short wavelength radiation sources"

7. REFERENCES

1. http://umbra.nascom.nasa.gov/eit/
2.http://trace.lmsal.com/
3. J. Zhu, Z. Wang, Z. Zhang, F. Wang, H. Wang, W. Wu, S. Zhang, D. Xu, L. Chen, H. Zhou, T. Huo, M. Cui and Y. Zhao, "*High reflectivity multilayer for He-II radiation at 30.4 nm*" Applied Optics Vol. 47, issue 13 , pp C310-314, 2008.
4. S. Zuccon, D. Garoli, M.G. Pelizzo, P. Nicolosi, S. Fineschi and D. Windt, "Multilayer coating for multiband spectral observations", in Proceedings of the International Conference on Space Optics (ICSO), ESA-SP (European Space Agency, 2006).
5. J. Gautier, F. Delmotte, M. Roulliay, F. Bridou, M.F. Ravet, and A. Jérome, "*Study of normal incidence of three-component multilayer mirrors in the range 20-40 nm*" Applied Optics Vol. 44, pp 384-390, 2005.
6. M. Suman, M.-G. Pelizzo, P. Nicolosi, and D. L. Windt**, "***Aperiodic multilayers with enhanced reflectivity for extreme ultraviolet lithography*", Applied Optics, Vol. 47, Issue 16, pp. 2906-2914.
7. D. L. Windt, Computers in Physics, 12, 360-370 (1998).
8. http://www.goes-r.gov/
9. C. Tarrio, R. N. Watts, T. B. Lucatorto, J. M. Slaughter, C. M. Falco, "*Optical constants of in situ-deposited films of important extreme-ultraviolet multilayer mirror materials*", Applied Optics, Vol. 37, pp.4100-4104 (1998).
10. D. L. Windt and W. K. Waskiewicz, "*Multilayer facilities for EUV lithography*", Journal of Vacuum Science Technology B 12, 3826-3832 (1994).